Manuscript number: amt-2022-215

Full title: "Consistency test of precipitating ice cloud retrieval properties obtained from the observations of different instruments operating at Dome-C (Antarctica)"

This is a very interesting paper that describes a unique set of instrumentation at a site in Antarctica that take data useful for studying ice clouds without supervision. The instrumentation consists of a Fourier transform spectroradiometer (REFIR-PAD), a depolarization lidar, and a micro-rain radar (MMR). From my own experience with satellite imager-based observations of ice clouds over polar regions, the retrievals are problematic and the issue is having some sort of ground truth with which to assess them. The methodology described in this article provides a very important step towards being able to provide a "truth" set for satellite-based comparisons, at least from my own limited perspective.

The paper would benefit from more work on the results section and revisions to some of the figures before publication. Suggestions for improving the grammar are provided in an uploaded edited version of the manuscript. Further suggestions are provided below for the authors to consider.

Major comment:

The data provided by the instrumentation at Dome-C could be very instrumental for improving the retrieval/description of precipitating ice cloud properties in the Antarctic. If there were retrievals at the time of polar-orbiting imager overpasses, the intercomparisons would be useful to a broad remote sensing community. The manuscript would be strengthened by making the case for how much data are needed and what might be necessary for increasing the quantity and reliability of the products. How much data are needed over how long a time period? Are results available every day? Is the data processing fully automated? Are the products available to the scientific community? What is the daily coverage? How would you improve the analysis given more data? In other words, make the case for what you are doing here and what would be gained by continuing this data collection and analysis effort. There are four case studies provided - how many more cases are necessary for your goals? More clarity of the current and future effort and goals should be provided, given that this manuscript will be referred to in future work.

We thank the reviewer for the constructive comments which gave us the opportunity to improve our paper. We have worked trying to address all requests.

During the 18 days accounted for in the analysis, a total number of 678 REFIR-PAD measurements colocated with MRR observations are considered. This dataset covers a very small time frame which does not allow an accurate evaluation of satellite sensor performances due to the scarcity of nadir collocated overpasses.
Nevertheless, collocated satellite passive measurements at any observational zenith angle are examined to investigate the opportunity of accounting for additional information in the analysis. For the present case the Infrared Atmospheric Sounding Interferometer (IASI, https://www.eumetsat.int/iasi) and the Moderate Resolution Imaging Spectroradiometer (MODIS, https://modis.gsfc.nasa.gov) are considered. The analysis of the L2 satellite products for IASI (https://www-cdn.eumetsat.int/files/2020-12/IASI%20Level%202_%20Product%20Generation%20Specification.pdf) and MODIS (https://atmosphere-imager.gsfc.nasa.gov/sites/default/files/ModAtmo/MOD06-ATBD_2015_05_01_2.pdf) highlights the difficulties in identifying the cloudy conditions, which

are otherwise determined by the ground-based sensors. In case of IASI the cloudy conditions are individuated in 55% of the 131 collocated observations while MODIS classifies as cloudy the 38% of the collocated 73 pixels. Moreover, given the low confident classification no cloud properties retrieval is available for the considered cases.
We totally agree with the reviewer that the use of ground-based observations can be used as truth to assess the capability of satellite sensor to identify atmospheric conditions and their retrieval products. Nevertheless, since long records from ground-based measurements are required to test L2 satellite products when strict co-location constrains are set, we preferred to not include this analysis in the present work.
For your information, we are performing a comparison between satellite (passive and active) L2 products with ground-based derived products (at Dome-C) on an extended time frame. Preliminary results are showing significant differences among multiple satellite sensors performances; it is our hope to submit our findings in a very near future.

Most of the instrumentation used in this work operates in continuous and unattended mode at Dome-C. In particular, REFIR-PAD provides an infrared spectrum every 12 minutes, while the MRR and the lidar provide measurements every 1 and 10 minutes, respectively. HALO-CAMERA acquires continuously since 2020 but it does not work during the winter period when the moon is not present. ICE-CAMERA performs a scanning of the precipitating ice crystals hourly, because it requires more time to complete all needed operations. Unfortunately, data were not always available because of some problematic related to this kind of measurements. In fact, for example the accumulation of the ice on the screen obstructs the scanning plate and makes it necessary to clean it before start measuring over. This procedure requires the intervention of the Concordia staff if it happens during the Antarctic winter period. This is why only four cases were discussed in detail in the paper, since they correspond to those days when also the ICE- or HALO-CAMERA images were available for the comparison with the retrieval products. Basically, REFIR-PAD, lidar and MRR provide continuous measurements every day, while ICE/HALO-CAMERA are actually not available every days due to occasional technical issues of maintenance.

We agree with the reviewer that more data would improve the analysis, in particular the comparison between Z_e retrieved from the REFIR-PAD spectral radiances and those measured by the MRR would be enhanced and made more reliable by collecting a larger number of measurements. This is the reason we need to continue the work by acquiring more data at Dome-C. However, the results shown in the paper prove that the methodology discussed is valid for the assessment of the particles size distribution at Concordia in case of precipitating ice clouds and it also shows the goodness of the retrieval procedure of the ice/mixed cloud optical properties from the infrared spectra in these conditions.
The following sentence was added in the Conclusions:
"We are confident that by extending the analysis of at least five more years the results would gain in quality and reliability. Furthemore, still within future perspective, the possibility of collect more retrieval of effective size of the precipitating crystals together with the Doppler velocity provided by the MRR, could allow to derive a new analytic relationship between the particle fall velocity and diameters, which is still missing for ice crystals as far as we know. This relationship could be used to directly estimate the size distribution from the radar power spectra".

Even though the retrieval products of precipitating ice clouds are clearly not always available every days, because these events are not so frequent and the MRR is sensitive only to the larger particles, the retrieval products of not precipitating events are available everyday. In fact, the routine of the analysis is fully automated and provides the retrieval products of the atmospheric profiles and clouds parameters continuously.

The products will be available to the scientific community within a partnership of scientific collaboration. The PNRA projects provide that the collected data will be available to the scientific community one year after they will be concluded.

We added the following sentences in the text on line 100:
“It was installed on the roof of the PHYSICS shelter in a zenith-looking observation geometry providing one measurement every minute”.

On line 115 :
“The photographs are analyzed to sort and classify the precipitating ice crystals depending on their habit and sizes and they are hourly provided unless work of maintenance or cleaning are needed causing a lack of data”.

on line 120 :
“HALO-CAMERA is a sky imager installed on the shelter roof since 2019 operating mostly continuously used...“

Minor comments:

The verb tenses change often in the manuscript - suggest aiming for as much consistency as possible.

Corrected in the text

Introduction, line 20: please define the term cloud effect and perhaps cloud forcing, which is used in line 54. That is, describe the components of the radiation budget in broad terms for the reader.

On line 20:
We replaced “Cloud effect can be either ...” with “Clouds can be responsible either of a net cooling... “

On line 29:
“The radiative forcing caused by these clouds, defined as the differences between the total flux in the presence of cloud and one in clear sky condition (Intrieri et al. 2002), influences the Surface Radiation Budget .. ”

Line 150: The figure - be specific about which figure is being referred to here.

Corrected in the text.

Figure 6: there are basically two figures set side-by-side in Figure 6, and the details are difficult to see in the left plot (panels a through d). Would it be possible to separate the two panels so that the details are easier to discern?

Figures were separated.

Lines 166-170: the description of realistic ice particles from this area (Dome-C) is quite interesting, and I would hope that the authors will consider expanding their interpretation of the observations from the ICE-CAMERA photographs, especially in precipitating conditions for the case study dates.

As suggested by the reviewer we widely extended sections 4.3.1 and 4.3.2.
From now on the figure numbers refer to those in the text. Regarding section 4.3.1:

"The MRR reflectivity time-height cross-section for the selected days 23 and 24 February 2020 are shown on the upper panels of Figs. 16 and 17. The data are not continuous because of the filtering procedure due to the sensitivity of the MRR to the largest particles. The corresponding color map of the backscattering and depolarization lidar signals are also shown on the right of Fig. 16. The depolarization lidar shows that precipitation starts from the passage of ice clouds between 02:00-04:00 UTC, when larger ice crystals formed as detected by the MRR signal, which reached a few dBZ above 0. Then the precipitations continued but with smallest particles, in fact the MRR signal decreases rapidly. On 24 February an intense precipitation started at 07:00 UTC and finished at about 22:00 UTC; this was composed of larger crystals as clear from the MRR signal in the upper panel of Fig. 17, in particular the signal reached about 3 dBZ at 11:30, 14:30 and 18:30 UTC. Fig.15 also shows the comparison of the average crystal length L_{av} retrieved from REFIR-PAD infrared spectra (red diamonds) with those obtained from the ICE-CAMERA (blue dots). Continuous MRR measurements and ICE-CAMERA data were available most of the time of both days as shown in Fig. 14.

Mixed-phase clouds passed above the site on 23 February between 08:00-09:00 UTC and 12:00-13:00 UTC, when their presence was detected by the lidar depolarization signal at around 200 m above the ground (indicated with black arrows) and, in particular, the supercooled water formed layers of 100 m and 300 m of thickness on the 23 and 24 February, respectively. The average retrieved precipitable water vapor (PWV) was found equal to 1.33 and 0.98 mm on the days 23 and 24 February, respectively, while the average cloud temperatures about -40 and -39 °C. The average temperature of the water layers was found equal to -31 °C, which is acceptable since supercooled water can exist down to -40 °C.
In the first mixed-phase cloud time slot, the retrieval provided an average ice fraction γ equal to 0.47 with LWP equal to 0.62 g/m^2 while in the second time slot values were equal to 0.56 and 1.5 g/m^2.

The lower panels in Figs. 14 and 15 indicate that the values of the average crystal lengths retrieved from REFIR-PAD and those estimated from ICE-CAMERA varied between 700–1200 μm and 700-1000 μm, respectively, and they are mostly in very good agreement for most of the cases, particularly on day 23 February.

Figs. 18 and 19 show the photographs took by the ICE-CAMERA at 04:10 UTC and 08:10 UTC on the days 23 and 24 February 2020, respectively. These times were selected because were close to the strong precipitations detected both by the lidar and the radar, as we can note from Figs. 16 and 17, when the sun was still rised and generating the halos. In Fig. 20 is also shown the photograph at the 18:03 UTC of the 24 February right before the intense precipitation detected by the lidar and radar (Fig. 17), where we can see the presence of columns aggregates (or clusters) and rimmed rosettes beside the hexagonal columns. The crystal habits were automatically catalogued by the internal algorithm, and labeled with the green labels. The solid column crystal are represented by hexagonal columns (label hexpri) or bullet (label bullet), which are columns with a tip at one end; aggregates (irrgra, clusters) were also found, together with bullet rosettes (rosette) or rimed rosettes (rimros). In general, some elements needed to be discarded since represent volatile material (label fiberr) produced by the main building of the station.

Ice crystal shown in Fig. 18 on the day 23 February indicate that almost only column-like crystals were present. On the contrary, the photograph in Fig. 19 on the day 24 February, shows also a little component of bullet rosettes.

The prevalence of hexagonal columns was confirmed by the detection of well distinguishable solar halos in the HALO-CAMERA images at the same times as shown in Fig. 21 for the both mentioned days. In fact, the right panel shows that the phase functions of the smooth columns, aggregate and bullet rosettes (σ_r = 0) present a strong scattering peak at 22 °, which is responsible for the most intense halos, while for the roughest particles (σ_r = 0.50) the function is smoother without the peaks: the parameter σ_r reported in Fig. 21 indicates the degree of rougheness with larger values denoting rougher particle surfaces, in particular, values 0 (smooth surface), 0.03 (moderate roughness) and 0.50 (severe roughness) were assumed as described in Yang et al. (2013). Since, as found by Forster et al. (2022), plate-like and hexagonal column-like crystal have a SCF (smooth crystal fraction) higher than solid bullet rosettes and columns aggregates, as also confirmed by the measurements performed by Lawson et al. (2006) at South Pole, the presence of the 22 ° confirmed the high occurrence of hexagonal columns".

We also added on the right side of Fig. 18, beside the halos images, the plot of the simulated phase functions at 532 nm of columns, aggregates and bullet rosettes with different grade of roughness as shown here below in Fig.1:

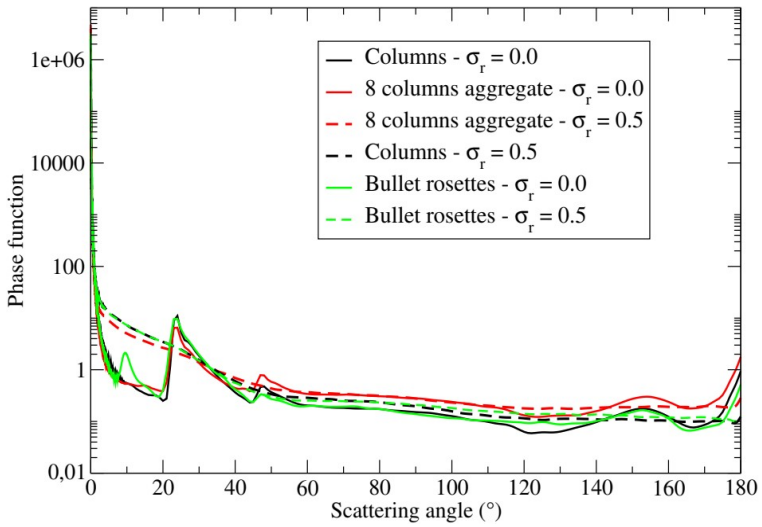

Fig. 1. *HALO-CAMERA images for the days 23 (left) and 24 (middle) February 2020. On the right panel the simulated phase functions at 532 nm for the three habits considered with roughness σ_r = 0 (smooth crystal surface) and σ_r = 0.5 (severe rough crystal surface).*

Regarding section 4.3.2:

"During 21 April 2020, strong precipitiations occurred between 08:00-15:00 UTC and between 17:00-24:00 UTC as we can see from the lidar signal on the lower panel of Fig. 22, while the radar reflectivity reachead 5 dBZ. The larger particles formed between 18:00-21:00 UTC as detected by MRR in the upper panel of Fig. 22. On 24 April, an intense precipitation detected by the backscattering lidar started at 03:00 UTC and continued until 15:00 UTC, while the MRR detected the Doppler signal from 05:30 UTC up to 11:00 UTC showing a strong reflectivity signal around 10:00 UTC.

Some photographs from ICE-CAMERA were available for the comparison as shown in the lower panels of Fig. 24 and 25. Unfortunately, on the 23rd, only a single ice scan measurement was

actually provided by the ICE-CAMERA at 03:03 UTC and it did not overlap in time with the radar data. However, the comparison of the 21 April shows a good agreement with the retrieved L_{av}. The MRR reflectivity shows high signal values, up to 8 dBz, between 19:00-21:00 UTC on 21 April and between the 06:00-11:00 UTC on 23 April.
Also during 21 April, a mixed-phase cloud with supercooled water occurred between 19:00 and 20:00 UTC at about 200 m above the ground.

The average retrieved precipitable water vapor (PWV) was found as higher as 2.46 mm for the day 21 April and 1.33 mm on 23 April, while the average cloud temperatures was equal to about -33 and -38 °C, respectively. The average temperature of the water layer occurred during the REFIR-PAD and MRR measurements was found equal to -23 °C and it was placed between 200 and 500 m above the ground. In this case γ was found on average equal to 0.58 and LWP equal to 9.5 g/m^2.

From ICE-CAMERA photograph in Fig. 24 we can see that on day 21 April at 19:03 UTC, in the middle of the second precipitation when mixed clouds passed, mostly columnar habits with a minor component of rosettes was present. On 24 April at 03:03 UTC, when the precipitation started and 1 hour and half before the MRR signal was detected, the falling ice crystals were mostly rosettes, as clear from ICE-CAMERA photograph shown in Fig. 25. Unfortunately, for these days the HALO-CAMERA images were not available".

Figure 10: Despite reading multiple times through the discussion pertinent to the results in this figure, it is difficult for me to interpret the comparison between REFIR-PAD and MRR of the intercept (No) and the optical depth since the results are on a log-log scale. There is a very wide range of results especially in the OD. Are there conditions where the results might compare more closely? Would results collected over a long time period be used to improve the retrieval process? Some discussion would be helpful here.

We agree. We have updated Fig. 10 by showing only the plot of D_{ei}-OD_i. We used a linear scale for the effective diameters. We added Fig. 2 (now Fig. 11 in the text) to show the variability of the retrieved ODs and their effect on the spectral radiances.

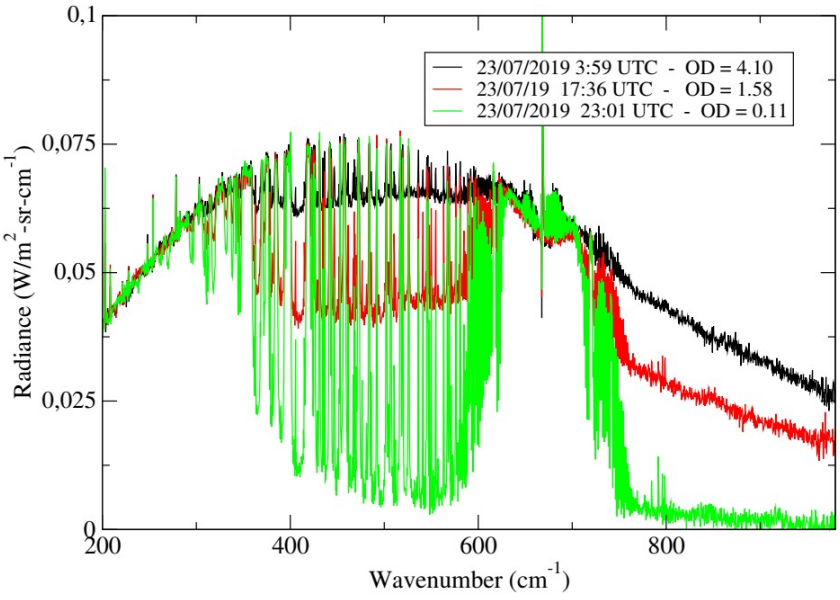

Fig. 2. *Variability of the cloudy spectra detected by REFIR-PAD during the day 23 July 2019.*

We added the plots in Fig. 5 (now Fig. 14 in the text) of the N_o expressed in cm^{-5} and the slope $\Lambda=(\mu+3)/L_m$ in cm^{-1} as a function of the cloud temperature (T_{cld}) to compare them with the results shown in Heymsfield et al. (2013, 2002) and Wolf et al. (2019), finding a good accordance.

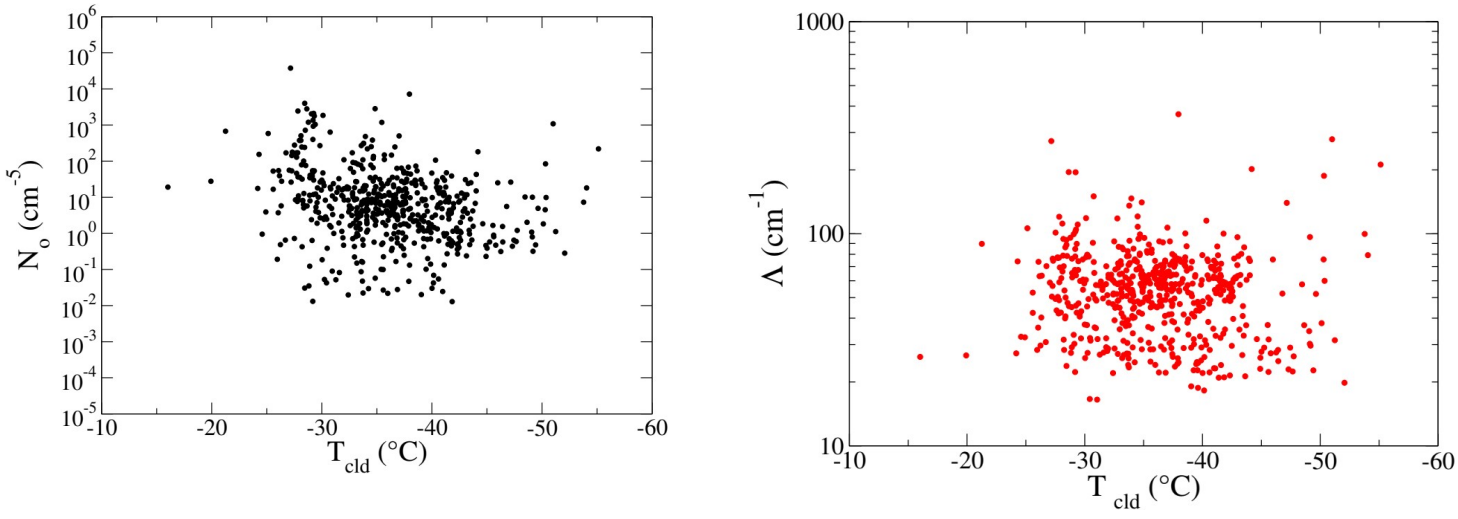

<u>Figure 5</u>. Left and right panels: intercept N_o and slope Λ as a function of the cloud retrieved temperature (T_{cld}).

Figure 12: For ease of interpretation for the reader, I think it would be helpful to break this figure into two different figures, one for each day. Perhaps consider making a 2-panel plot of the MRR reflectivity map above/below the lidar map for each day so that the figure is expanded to help interpretation. Another suggestion would be to draw a circle around the times when a supercooled liquid water cloud is present in the lidar map. My final suggestion would be to expand the discussion for each day to focus on results at different times through the day, i.e., describe the results in more detail. How does the MRR add information to the REFIR-PAD results?

We have implemented all changes suggested by the reviewer.
The MRR allowed to confirm the goodness of the retrievals of the PSD parameters (intercept and modal radius) from REFIR-PAD spectra, assuming the dispersion coefficient μ = 0,1,2. We have now assumed these range of values because of the dependence of this parameter on the cloud temperature as suggested by reviewer 2 and discussed in detail in Heymsfield et al. (2013, 2002). The results of the cloud parameters retrieval do not depend on the choice of μ since the downwelling infrared spectra detected by REFIR-PAD are not sensitive to this parameter as shown and discussed in detail in the answers to reviewer 2. However, the N_o change a little and need to be recalculated. Results of N_o and slope Λ are shown above in Fig. 5 as a function of the retrieved cloud temperature. Fig. 7 was updated by using μ = 1.
Then, MRR reflectivity data also allowed to assess which types of crystal habits better fit the measurements, finding that the best accordance is found mostly by assuming hexagonal columns and aggregates and, in smaller amount, bullet rosettes.

Figure 13: As noted earlier, the ice particle habit observations by the camera are quite interesting. Unfortunately, this figure shows exceptionally small images for two different days. It is difficult to make out any detail because the images are so small. Please

consider reworking these figures, perhaps making a separate figure for each day with fewer (but larger) ice particle images. It would also be of interest to discuss what habits are found for each of the case study dates, under the specific conditions of the day (temperature/humidity), and pointing to specific images. This is an important component of your analyses but these figures are not helpful.

We have separated all the figures requested. We also added in the section 4.3 the specific conditions of average temperature and precipitable water vapour for all cases.

Figure 15: same general comment as with Figure 12. Please consider separating this into two figures, one for each day. Furthermore, there is almost no interpretation of the results for these two days (21 and 23 April 2020) - the discussion should be expanded.

Figures were separated and discussion was expanded as suggested.

Figure 16: same general comments as for Figure 13. It is difficult to get any information from these images of the ice particles. But the images should be useful for supporting the analysis in Figure 15.

Section was expanded in the manuscript.

We have also applied the grama corrections suggested by the reviewer, in particular by uniforming the tense as much as possible.

Manuscript number: amt-2022-215

Full title: "Consistency test of precipitating ice cloud retrieval properties obtained from the observations of different instruments operating at Dome-C (Antarctica)"

This is an interesting article that uses REFIR-PAD Fourier transform spectroradiometer, MMR,lidar data and particle probe imagery for four case studies of precipitating ice clouds at Dome-C,Antarctica. The REFIR-PAD data are forward modeled to retrieve microphysical properties of the clouds, and then the results are compared to the MRR reflectivity data. The methodology described in this article provides ground-truth for satellite-based retrievals of ice cloud properties in Antartica. I recommend considering my comments and modify the article appropriately before the article is accepted.

Main Comments

1. I'd like to see a sounding, or at the minimum, discussing the temperatures sampled for each of the four cases. This should be done in the abstract as well as in the body of the text.

We thank the reviewer for the constructive comments and advises, which allowed improving the quality of both our analysis and the manuscript. We tried to address all requests.

The temperature profile during the precipitation events usually varied from -20 °C to -40 °C. The average temperature obtained by weighting the retrieved profiles over the entire dataset with the corresponding backscattering lidar signal was found equal to -28 °C. We showed in Fig. 1 the plot of four retrieved profiles of temperature (colored lines on the left panel) at the dates reported in the label. We can see the inversion of the temperature, typical of the Antarctic Plateau, at around 750 m above the ground, while the strong peak at the very first layers corresponds to the internal temperature of the REFIR-PAD instrument, since this latter was treated as a separated environment in the retrieval procedure as also mentioned in the text. We can also see that only on 21/04/2020 the inversion of the temperature reached the -6 °C at around 1000 m.
On the right panel, we have also reported the backscattering lidar profiles, which show that the precipitating clouds occurred below 500 m, so that the average temperature weighted with the lidar signal turned out being equal to -30 °C on the days 23/02, 24/02 and 23/04, while it rised up to -25 °C on the day 21/04.

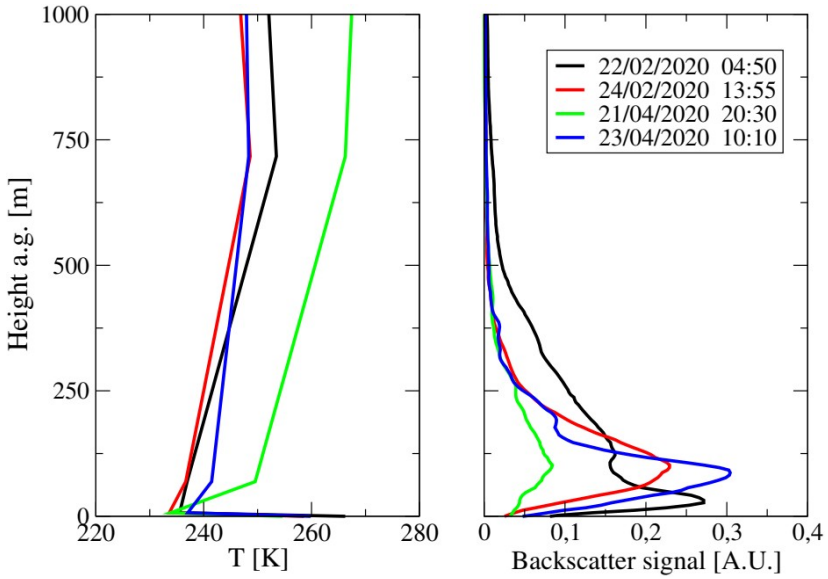

Figure 1. *Left panel: retrieved temperature profiles corresponding to the selected days of measurement. Right panel: backscattering lidar signals in arbitrary units for the analysed measurements.*

The average temperature values and Fig. 1 were both added in the abstract on line 9: "*The retrieved effective sizes and optical depths varies on average in the range 100 - 200 μm and 0.1 - 5, respectively. The average in-cloud retrieved temperature over all dataset was found to be -28 °C*". The following sentence was added to the text at line 339 : "*The retrieved effective diameters mostly varied in the range 100-200 μm, while the retrieved optical depth between 0.1-5 over all dataset. From the retrieved temperature profiles we assessed the average in-cloud temperatures by weighting the profiles with the corresponding backscattering lidar signals. The temperature varied between -20 °C and -40 °C and on average was equal to -28 °C. Specifically for the cases discussed hereafter, the average temperatures turned out to be -30 °C on the days 23/02, 24/02 and 23/04, while on the day 21/04 equal to -25 °C"*.
Daily radiosondes were routinely launched at Concordia station at 12:00 UTC by the Italian meteo Climatological Antarctic Observatory staff. This data, since were not continuous, most of the time they were not available at the time of the REFIR-PAD measurement. However, they allowed to obtain a good climatology of the atmospheric profile used as a priori information and initial guess in the retrieval procedure.

2. An opportunity was missed to combine the MRR and Lidar data to derive the microphysical properties of the clouds sampled, using retrieval algorithms such as 2CICE, DARDAR and its successor. As it stands, the lidar data is not used for the analysis, maybe just to determine liquid water presence (?) and for the plots shown.

We know well the two methods mentioned by the reviewer. They exploit the synergistic combination of radar-lidar observations, but their effectiveness is limited to a radar signal at higher frequencies than that of MRR (24 GHz, K band). As far as we know, these methodologies have been largely applied only to the satellite measurements, such as CLOUDSAT-CALIPSO (DeLanoe and Hogan (2008/2010) by using the DARDAR algorithm and Deng et al. (2015) by using the 2C-ICE). In both these cases the signal of the CPR Radar at 94 GHz (W band) was exploited, which was sufficiently high to explore the smallest particles and sensitive to the top of the clouds, where no precipitation events can occur. This allows addressing stable solutions within the retrieval algorithm. In our ground-based configuration, the MRR is a radar that presents strong limits in sensitivity and furthermore is used from the ground and very close to the precipitation.
On the other hand, the backscattering-depolarization lidar installed at Dome-C provides only qualitative measurements and it also shows clear limits in the performance, in fact the generated signal turns out to be too noisy, mostly in the height near above the cloud top, to be used in any kind of retrieval algorithm, such as the Klett inversion method as we done, for example, during FIRMOS campaign at Zugspitze mount (Di Natale et al. 2021). We have already tried to apply this method in order to derive the cloud extinction profile and, thus, the optical depth, but every attempt has failed so far as expected. We added the following sentence to the text on line 271 in order to clarify this aspect: " *A direct retrieval of the optical extinction or ice fraction from the lidar measerements was not possible due to the high noise of the signal above the cloud top heights, which does not allow the application of a retrieval algorithm such as the Klett method. These lidar measurements represent qualitative data, which allow identifying the occurrence of clouds and assessing their position and the presence of ice and supercooled water. "* .

3. You could use the lidar data in the following way. Convert backscatter to extinction. Then, use the relationship between ice water content and extinction from the following article and those used in the study: Thornberry, T. D., Rollins, A. W., Avery, M. A., Woods,

S., Lawson, R. P., Bui, T. V., and Gao, R.-S. (2017), Ice water content-extinction relationships and effective diameter for TTL cirrus derived from in situ measurements during ATTREX 2014, J. Geophys. Res. Atmos., 122, 4494– 4507, doi:10.1002/2016JD025948.

As we stated by answering the previous comment, the backscattering-depolarization lidar installed at Dome-C provides qualitative measurements, which allow to well identify the occurrence of clouds and precipitation events, to derive the cloud position (top and bottom heights) and to detect the presence of supercooled liquid water. The retrieval of the extinction profile and, thus, the optical depth, as well as the ice fraction liquid/ice is quantitatively not possible to achieve by using this lidar data.

4. The data from the ICE Camera offers an opportunity to derive particle masses from the melted diameter. The heated glass plate the particle land on provides that opportunity- initial diameter and melted diameter. The melted diameter may not be spherical but laboratory experiments could be conducted to find the relationship between melted diameter and spherical diameter.

The ice particles never melt on the ICE-CAMERA surface, as its temperature is kept below -5 °C also during the heating of the plate. Sublimation occurs without melting. This information was added to the text.

5. The Doppler velocity data from MRR could be used to derive the median mass diameter.

Median mass diameter could be inferred from Doppler velocity observations by MRR, but this requires a relationship between diameters and velocities of the falling particles. While this relationship is relatively fixed for liquid precipitation (and MRR exploits it to obtain DSDs for each probed height during rainfall), the solid hydrometeors can follow different v-D relationships due to their sizeable microphysical variability (habits, shapes, orientation, fall behavior, and density).
As a follow-on of this article, we plan to combine radiometer and MRR Doppler data to achieve a v-D relationship (or more relationships) suited for DC precipitation, even combing observations from the ICE-CAMERA and from a disdrometer to be installed soon. Nevertheless, this analysis needs more snowfall data to make the finding more robust. This is the reason why we have not derived particle diameters from MRR data at this stage, but this analysis will be performed in a future work.

6. The PSD dispersion is given as 7 on line 138. I suggest using a temperature-dependent dispersion, such as given in the article Ice Cloud Particle Size Distributions and Pressure-Dependent Terminal Velocities from In Situ Observations at Temperatures from 0 to -86C by .

We are grateful to the reviewer for this hint.
Referring to the paper Heymsfield et al. (2002, 2013), Wolf et al. (2019) and Jackson et al. (2015) (all these references were added to the manuscript), according to the range of temperature found at Dome-C from our analysis, between -50 and -25 °C, the values of the corresponding μ coefficient of the PSD should span between 0 and 2.
From a radiometric point of view, as already discussed in Wyser and Yang (1998), if we have defined the effective diameter as in Eq. (2) in the text, the spectral radiance turns out to be insensitive to the detailed shape of the size distribution, in particular to the dispersion coefficient μ. We showed in Fig. 2 the plots of the differences between the spectral radiances simulated with SACR by placing ice clouds from the ground up to 5 km of absolute height with optical depths 0.2, 0.8, 1.5 and 4, and effective diameters equal to 100 and 200 μm, as they cover the range of values found; simulations were performed by averaging the single scattering properties provided by the

Ping Yang database by using three different dispersion coefficients μ, namely 0, 2 and 7. In red are shown the differences between the radiances simulated with μ = 0 and μ = 7 (the value used in our analysis), rather in green are shown the differences between the radiances simulated with μ = 2 and μ = 7. The black curves represent the REFIR-PAD spectral noise. We can see that the differences are well inside the noise also in the far infrared (FIR), though downwelling spectral radiance is not sensitive to the detailed shape of the PSD, and the value of μ does not affect the results of the cloud parameters retrieval.
We added the following sentence to the text on line 143: "As long as the effective diameter is defined as in Eq. 2, the spectral radiance detected by REFIR-PAD turns out to be insensitive to the detailed shape of the size distribution, in particular to the dispersion coefficient μ. We also verified this assertion by performing simulations of the downwelling spectral radiance for different values of D_{ei} and OD_i by assuming different values of μ between 0 and 7 to generate the crystal infrared optical properties. So that the results of the cloud properties retrieval can not be affected by the choice of μ.".

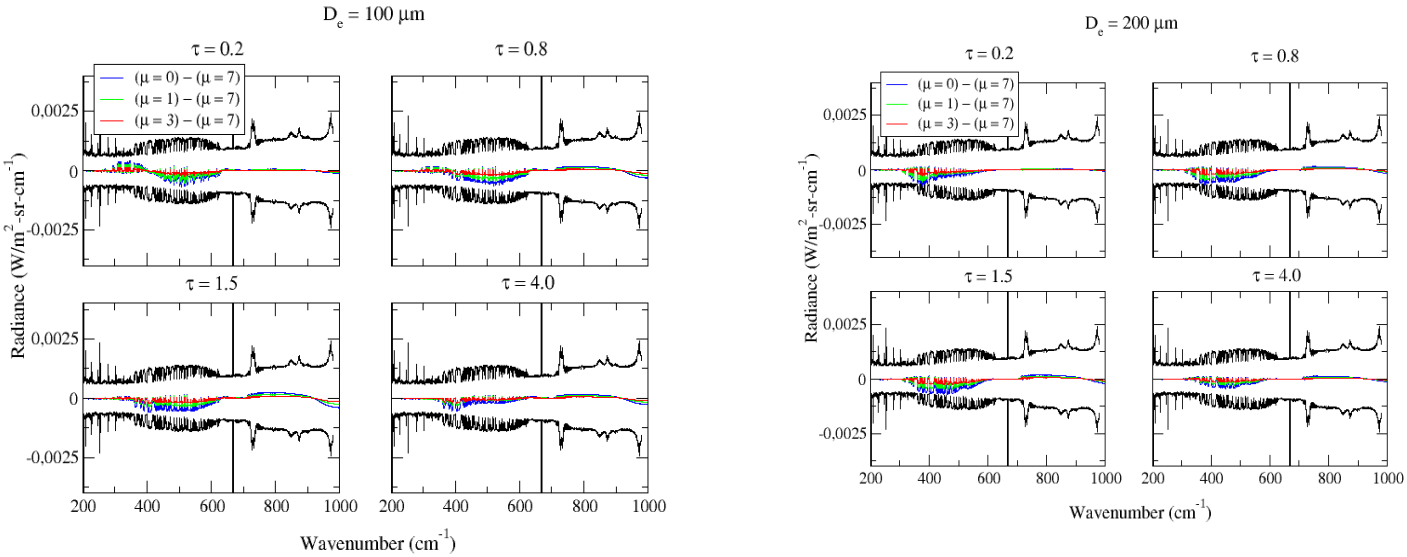

Figure 2. *Differences of the spectral radiances simulated with SACR by placing a precipitating ice cloud from the ground (3.233 km) up to 5 km of absolute height with optical depths 0.2, 0.8, 1.5 and 4, and effective diameters equal to 100 μm (left plot) and 200 μm (right plot); the single scattering properties provided by the Ping Yang et al. (2013) database were averaged by using three four dispersion coefficients, 0, 1,3 and 7. The differences between radiances obtained with μ = 0 and μ = 7 are represented by the blue curves, the differences between μ = 1 and μ = 7 are indicated by the green curves and those between μ = 3 and μ = 7 are reported in red. In black the REFIR-PAD spectral noise is also reported.*

We can conclude that the coefficient μ does not affect the retrieval results of cloud parameters OD_i and D_{ei}. However, the intercept N_o change a little and was recalculated by using Eq. 9 and expressed in cm^{-5} to compare it with the results by Heymsfield et al. (2002) and (2013). As a consequence, also the values of Z_e from Eq. 23 were updated. We also have updated Fig. 11. The values of N_o and the slope $\Lambda = (\mu+3)/L_m$ were shown in the new plots of Fig. 14 as a function of the cloud temperature T_{cld}. The N_o values varies between 10^{-2} and 10^{4} , while Λ between 20 and 200 cm^{-1}; these values turn out to be in very good agreement with the distributions found both in Heymsfield et al. (2002) and (2013).

We have replaced Table 1 with another one indicating only the habit indeces need for interpretating the plot in the added figure (Fig. 12) reported below.
"In Fig. 3 below (now Fig. 12 in the text), in the upper panel were reported the reduced χ^2_{red} obtained from the Z_e retrieved from REFIR-PAD and those measured by the MRR by assuming μ = 0,1,2 (green, blue, red curves); in the lower panel are shown the total number of measurements (N) available considering the cut off at -5 dBZ. On the x-axis we reported the habit index explained in Table 1. To select the best habits we adopted the criteria of having the χ^2_{red} close to 1 and maximixe the number of measurements (N) by assuming some thresholds (dashed black lines in Fig. 3): we required that N had to be greater than 25 and χ^2_{red} had to stay between 0.5 and 2, since when it decreases too much usually indicates that the error is overestimated. The selected cases that complied the criteria were identified with cyan triangles.
From Fig. 3 we can see that there is no much difference by varying μ in the range 0-2 for the selected cases, so that we assumed as average value μ = 1 for the next considerations.

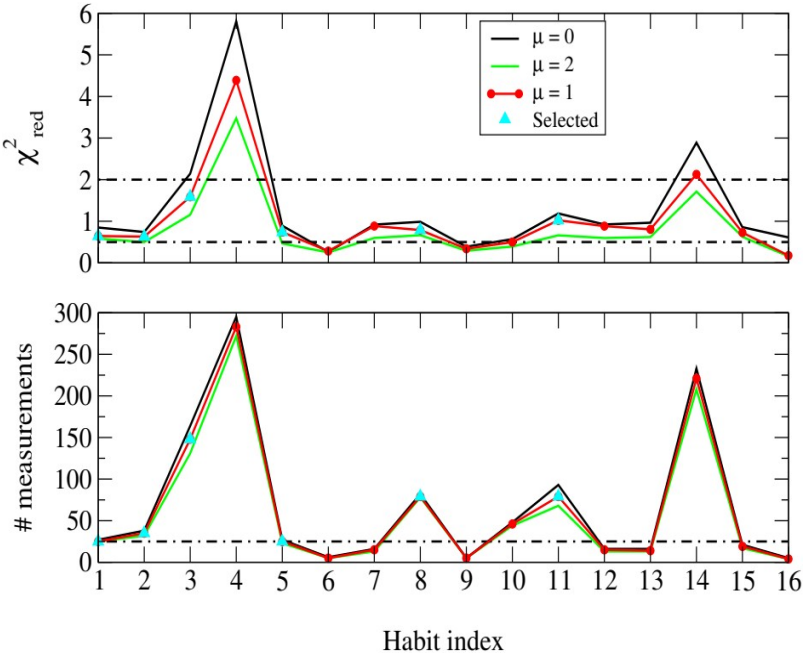

Figure 3. Upper panel: reduced χ^2_{red} calculated from the Z_e retrieved from REFIR-PAD and those measured by the MRR by assuming μ = 0,1,2 (green, blue, red curves). Lower panel: number of measurements above the -5 dBZ threshold assumed for the analysis.

The habits that showed best accordance with the radar measurements were the 5/6 branches bullet rosettes, the thin and long columns and the 8-columns/large block aggregates. Fig. 4 (now Fig. 13 in the text) shows the comparison of the MRR measured reflectivity with those obtained from REFIR-PAD by using some of the habits from the EMD (Eriksson Microwave Database) in Table 1 that provided the best agreement.
The high occurrence of hexagonal columns, aggregates and bullet rosettes was confirmed by the ICE-CAMERA photographs. In particular, the high occurrence of hexagonal columns was corroborated by the presence of 22° halos detected by the colocated HALO-CAMERA sky images as shown in previous studies at South Pole by Lawson et al. (2006).
It also should be noted that while the correlation coefficient turned out to be moderate (maximum ~0.3), this was mostly due to the difficulty of retrieving with good accuracy the shape of the PSD from the FIR observations, and in particular the intercept N_o , for large particle sizes, and mostly because of the need of increasing the number of measurements for improving the statistical distribution.

However, the results indicate that in the particle size range between about 600 and 2000 μm, the retrieval algorithm was able to estimate the intercept assuming the dispersion coefficient μ in the range 0-2, as shown in Fig. 4. The distributions of the retrieved N_o converted in cm^{-5} and the slope $\Lambda = (3+\mu)/L_m$ in cm^{-1} as a function of the retrieved cloud temperature (T_{cld}), were found in very good accordance with those found in Heymsfield et al. (2013, 2002) and Wolf et al. (2019) and they were shown in Fig. 4, left and right panels, respectively. Note that N_o varied mostly between 10^{-2} – 10^4 cm^{-5}, while Λ mostly between 20-200 cm^{-1}. The average relative error found for N_o was equal to 20%, which was comparable to the systematic error due to the assumption of a specific habit in the retrieval as shown in Fig. 7."

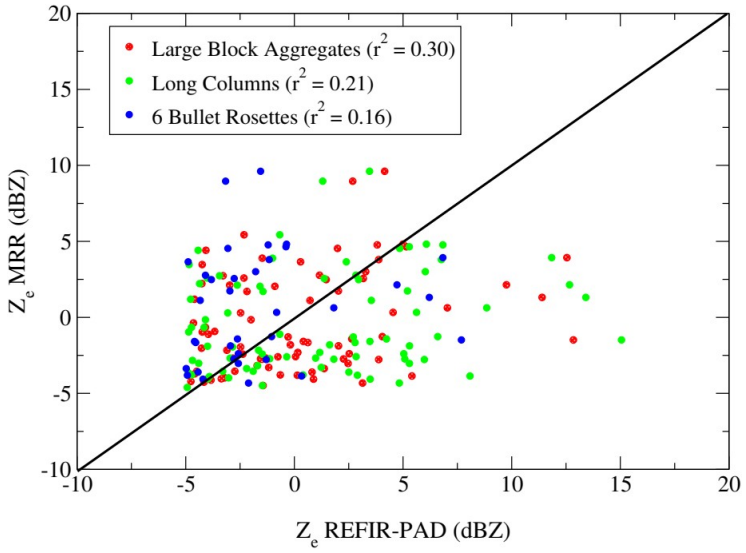

Figure 4. Scatter-plots of the Z_e measured by the MRR and those retrieved from REFIR-PAD by assuming μ = 1 and by using the habits from Eriksson et al. (2018) database that provided the best accordance: long columns, large plates aggregates and 6 bullet rosettes.

This results and updates were added in the text, abstract and conclusions.

Minor Comments

Reviewer R1 has noted improvements to the figures that should be made.

Yes, all the requests have been addressed.

Line 101. What are the minimum and maximum altitudes sampled by the MRR.

We have set MRR with 40 m as height resolution, so the sampled range goes from 40 to 1240 m. However, the first two range gates are usually excluded as they are affected by near-field effects, likewise the last range gate due to the low SNR. So, the actual MRR altitude range is 120-1200 m.

102-103. What are the minimum and maximum reflectivities that can be measured by MRR?

The manufacturer indicates -2 dBZ as the minimum detectable reflectivity for MRR. In this work, we have applied the Maahn and Kollias' (2012) routine to MRR raw data to improve MRR

sensitivity measurements in case of snow. According to them this routine increases MRR sensitivity to −14 and −8 dBZ, depending on the vertical range bin. However, we discarded reflectivity values lower than -5 dBZ from the analysis since, below that threshold, MRR measurements could be incomplete. So we have adopted a very conservative threshold to preserve MRR data's reliability in a very challenging site such as Dome-C.

138-139. Compare your sigma and mu values to those observed for cirrus clouds.

Within the REFIR-PAD retrieval procedure, we assumed a PSD with a dispersion coefficient μ given by the relation μ = 7. This was assumed in previous work in the Arctic and in Antarctica, since there are no sufficient measurements in the latter place. However, following the reviewer advice, we reconsidered values of μ coefficient according to the statitistical relationship with the cloud temperature as discussed in Heymsfield et al. (2013, 2002), using the values 0, 1 and 2 to calculate the N_o and the radar reflectivity Z_e as provided in the mentioned works for temperatures between -25 and -50 °C. The rerieval products were not affected by changing μ, since the downwelling infrared spectrum is not sensitive to this parameter as shown in the Fig. 1. We added the plots in Fig. 5 (now Fig. 14 in the text) of the N_o expressed in cm^{-5} and the slope Λ in cm^{-1} as a function of the cloud temperature (T_{cld}) to compare them with the results shown in Heymsfield et al. (2013, 2002) and Wolf et. Al (2019), finding a good accordance for our range of temperature.

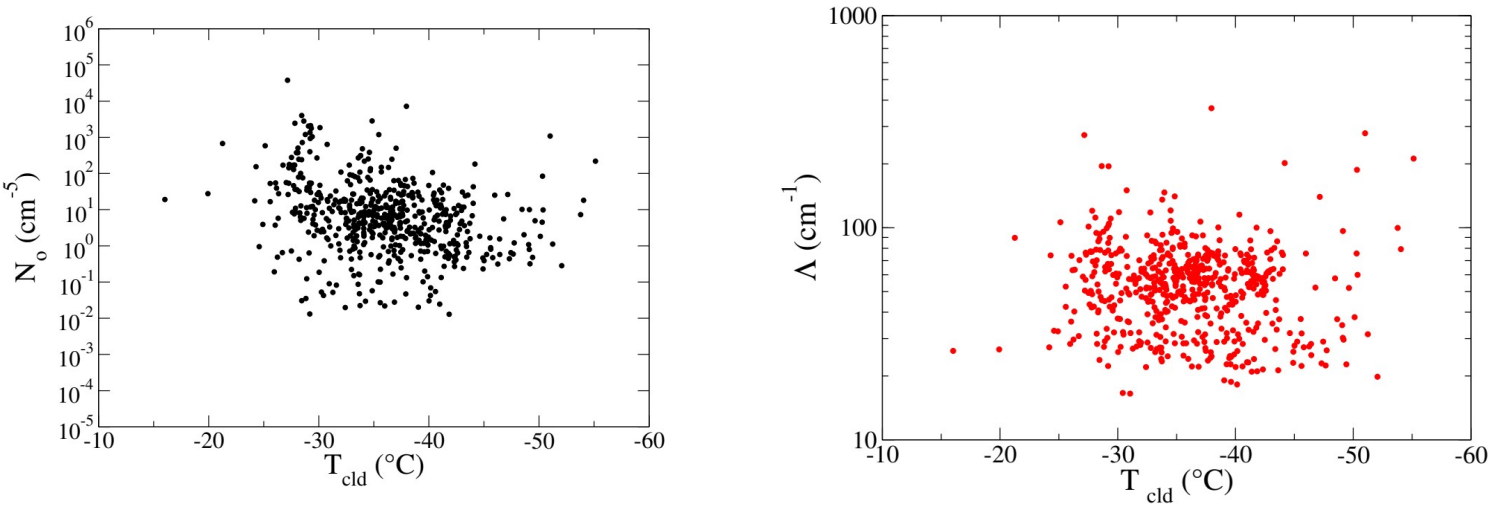

Figure 5. Left and right panels: intercept N_o and slope Λ as a function of the cloud retrieved temperature (T_{cld}).

164: "to us"

Corrected in the text.

166: Specifically, what are the temperatures of the clouds studied here.

The average cloud temperature was calculated by averaging the retrieved temperature profiles inside the cloud top and bottom weighted with the corresponding lidar signals and it was found equal to -28 °C. We added this value in the text.

216: How is liquid water detected from your instruments.

The liquid water and ice water path could be derived from the REFIR-PAD retrieval products by using Eq. (7) for water and ice.
Mixed-phase clouds appeared above the site on 23 February between 8-9 UTC and 12-13 UTC, where the presence of supercooled water was detected by the depolarization signal at around 200 m above the ground. In the first mixed-phase cloud time slot, the retrieval provided an average ice fraction γ equal to 0.47 with liquid water path equal to 0.62 g/m^2, while in the second time mixed-phase slot values were equal to 0.56 and 1.5 g/m^2.
On 21 April, a mixed-phase cloud with supercooled water occurred between 17 and 20 UTC at about 1500 and 400 m above the ground. In this case γ was found on average equal to 0.58 and LWP equal to 9.5 g/m^2.
These sentences were added to the text at lines 354 and 364, respectively.
On the advice of reviewer 1 we also expanded the discussion about the results shown in section 4.3.

262. You have particle imagery to characterize the particle habit(s). How does this compare to the particle types interpreted from the analysis.

The retrieval from REFIR-PAD infrared spectral radiances allowed to assess the D_e and, thus, the modal radius L_m of the PSD, which represents the main parameter to which the downwelling radiance turns out be sensitive. The other important parameter, the intercept N_o, was also derived from both the D_e and the optical depth OD_i. The cloud parameters retrieval from the REFIR-PAD infrared spectra is not affected by the specific value of μ, in fact the infrared downwelling spectral radiance is insensitive to it as the effective diameter is defined as in Eq. (2). To calculate the N_o from Eq. (9), we assumed μ = 1 and then we calculated the reflectivity. Retrieved reflectivity fit well the radar data even though a moderate spread occurs because of the difficult to precisely estimate the PSD parameters due to the assumption of homogeneous vertical size and habit distribution along the precipitating cloud and because more data need to be collected for improving the statistics. The photographs of the ICE-CAMERA clearly show the presence of estimated columns and aggregates in the cases 23-24 February (Figs. 18 and 20 in the text), while some bullet rosettes appear on 24 February at 8:00 UTC (Fig. 19 in the text). The figures of the ICE-CAMERA photographs were updated, as also requested by the reviewer 1: they were enlarged and we added the zoom on specific ice crystals.

310: "provided" to "provide"

Corrected in the text.

320: Specifically, what were the measured in-cloud temperatures?

We added in the text the values of the mean in-cloud temperature over all dataset, found equal to -28 °C, and the specific values corresponding to the four selected cases.

Figure 11: To me, the relationship between Ze measured by MRR and that retrieved does not look very good. MRR reflectivites are quite flat whereas those from REFIR-PAD vary quite a bit.

As we already stated, the sensitivity of the MRR is pretty low to the ice crystals occurring at Dome-C, in fact it allows to detect only the larger particles. The PSD retrieved from REFIR-PAD measurements decribes an average distribution of the particle sizes over all the precipitating clouds, which can turn out being affected by a large error. For this reason, we are aware that even though the retrieved points stay along the median line, a wide spread occurs between the data, indicating a moderate correlation index, as stated in the text. However, the fact that the values of the calulated Z_e and those measured by the radar are close and of the same order represents a good indicator of the

goodness of the retrieval of the PSD parameters and their consistency. Finally, we are confident that collecting more data will allow improving the correlation between the retrieved Z_e and the observed ones.

Figures 13 and 16: Show fewer crystals in Figs. 11-12 so that they can be more easily identified by the reader

We suppose the reviewer refers to the crystals of the ICE-CAMERA scannings in Fig. 13 and 16. In this case, we think that it would be better to split the two photographs as also suggested by the reviewer 1. In fact, we agree that some of the smallest crystals could be difficult to distinguish. Figures were separated, enlarged and we added the zoom on specific crystals.

360, 361: remove "the" in "between the"

Corrected in the text.

368. It would be nice to do some combined radar/lidar analysis or lidar analysis separately.

As discussed in the previous answers, a deeper analysis of the lidar data is not possible, since the signal turns out to be too noisy and it does not allow the application of a retrieval algorithm to derive the extinction coefficient and the optical depth. This is due to a limitation of the instrument which was made by prioritizing the compactness, portability, and durability in order to be installed in such an extreme site. For this reason, the data provided by this lidar are mostly qualitative and not quantitative. Similarly, the MRR is a compact object that exhibits clear limits in power and performance, but it also guarantees durability and reliability in such environmental conditions.

References:

[1] Julien Delanoë and Robin J. Hogan, “A variational scheme for retrieving ice cloud properties from combined radar, lidar, and infrared radiometer” , Journal of Geoph. Research, Vol. 113, D07204, doi:10.1029/2007JD009000, 2008.

[2] Julien Delanoë and Robin J. Hogan, “Combined CloudSat-CALIPSO-MODIS retrievals of the properties of ice clouds”, Journal of Geoph. Research, Vol. 115, D00H29, doi:10.1029/2009JD012346, 2010.

[3] Min Deng, Gerald. G. Mace, Zhien Wang, and Elizabeth Berry, “CloudSat 2C-ICE product update with a new Z_e parameterization in lidar-only region”, Journal of Geophysical Research: Atmospheres, Vol. 120, No. 23,doi:10.1002/2015JD023600, 2015.

[4] Maahn, M. and Kollias, P.: Improved Micro Rain Radar snow measurements using Doppler spectra post-processing, Atmospheric Measurement Techniques, 5, 2661–2673, https://doi.org/10.5194/amt-5-2661-2012, 2012.